We thank Reviewer #2 for his or her useful comments on our manuscript and appreciate the time and energy that must have been spent on this detailed review. All comments have been thoroughly considered so as to improve the manuscript. Hereafter Reviewers' comments are written in *black italics*, our responses in bold black fonts and the changes in the manuscript in blue bold.

This is a clearly-written and presented article showing key results of dust size distribution and optical properties measured over the Mediterranean during the ChArMEx/ADRIMED aircraft field campaign. The results add to the body of data building up to document dust properties and how they may change with transport, which can contribute to model and satellite retrieval validation and improvement. In particular the authors present results showing the minimal impact of pollution on dust properties, and retention of coarse mode particles which they attribute to turbulence in the dust layer. I recommend that this article is published, subject to some minor corrections, mainly concerned with further information on inlet impacts on sampling and size distributions, and some additional clarifications and additions to the figures.

Specific comments

R2.1. "Moderate light absorption" – which do you mean, moderate to light, moderate, or light? These are all different!
"Moderate" refered to the ability of particles to absorb light.
Updated text: "Moderate absorption of light by the dust plumes was observed with values of aerosol single scattering albedo at 530 nm ranging from 0.90 to 1.00 ± 0.04."

R2.2. "assumed similar" would be better than "assimilated" here
Thank you, this is corrected.

R2.3. 21610 L5-7 – and global transport of dust in general as well?
This is added in the text.
Updated text: "The results presented here add to the observational dataset necessary for evaluating the role of mineral dust on the regional climate and rainfall patterns in the western Mediterranean basin and understanding their atmospheric transport at global scale."

R2.4. Introduction – please give an overview of what is contained in each following section at the end of the introduction.
We now provide an overview of the different sections in the introduction.
Additional text: "Section 2 describes the aircraft strategy, the instrumentation and the method used to determine the aerosol size distribution, chemical composition and the associated optical properties. Section 3 presents the campaign meteorology, the dust vertical profiles and the results of the aerosol properties within the dust plumes. Section 4 explores the potential factors affecting the variability of the aerosol properties due to altitude and dust age. Section 5 concludes this article."

R2.5. Figure 1: Is it possible to change the aspect ratio of the figure so the landmasses appear more in proportion? Currently it appears squashed east-west.

The scale of the figure is changed.

R2.6. Some flight tracks/colours are not visible. Do some flight tracks overly others? E.g. F35, F38? If so describe this in the caption.
The colour codes of F35 and F38 are changed in order to better identify flight tracks in the figure.

R2.7. 21613 On what basis were the non-dust flights removed from the analysis?
Flights dedicated to the measurement of dust plumes were firstly planned using different dust plume forecast models, as explained in section 2.1. Sampling of mineral dust was then further confirmed by analysing satellite images and backward trajectories of the air masses, which are described in section 2.4. We add a sentence in section 2.1. to clarify it.
Additional text: "These flights were carefully selected to provide measurements of air masses from dust active sources based on the analysis of satellite images and backward trajectories, as described in section 2.4."

R2.8. L20-25 – what spatial distance is covered during a vertical profile?
This information is added in the text.
Updated text: "The general flight strategy consisted of two main parts: first, profiles from 300 m up to 6 km above sea level (asl) were conducted by performing a spiral trajectory 10-20 km wide to sound the vertical structure of the atmosphere and identify interesting dust layers. "

R2.9. Table 1 – I believe times should be in UTC for ACP papers.
Time are already expressed in UTC in Table 1, there was a typesetting error.
Updated text: "Times are expressed in Coordinated Universal Time (UTC)."

R2.10. Section 2.2.1 – It would be useful to define what the authors refer to by 'nominal size' here.
The definition is added in the text.
Updated text: The SMPS system provided the number size distribution of the electrical mobility diameter from the 30 - 400 nm in 135 nominal size classes (i.e. size classes provided by the instrument and not corrected for the dynamic shape factor) over time scans lasting 120 seconds.

R2.11. 21615 L10 – "possible errors in the FSSP sizing were assumed to be 30% of the particle diameter" – this sentence is confusing – do you mean errors in number concentration as a function of size? Please explain.
No, we referred to the measurement uncertainty in diameter. This is clarified in the text.
Updated text: The FSSP has an uncertainty in diameter of about 30 % according to Baumgardner et al. (1992).

R2.12. L14-15 – again, what do you mean precisely by 'particle sizing?'
This is clarified.
Updated text: According to the calibration of the GRIMM with standard, we assumed an uncertainty in diameter of 10%.

R2.13. 21618 L16 -21619, L7 – This (i.e. excluding data) is an interesting approach to the problem of scattering response vs size. It would be interesting to mention whether including the omitted data made much difference to the resulting size distribution? I.e. perhaps this approach is overly cautious.

Figure A compares the particle size distributions measured by the FSSP on its full size range with that obtained by the GRIMM for different dust layers sampled during the campaign. Systematic differences in the size distributions measured by the instruments can be seen around 2 µm most likely due to the fact that the light intensity response of the instruments is unique in this size range. Therefore we believe that datapoints obtained from the FSSP must be excluded from the analysis.

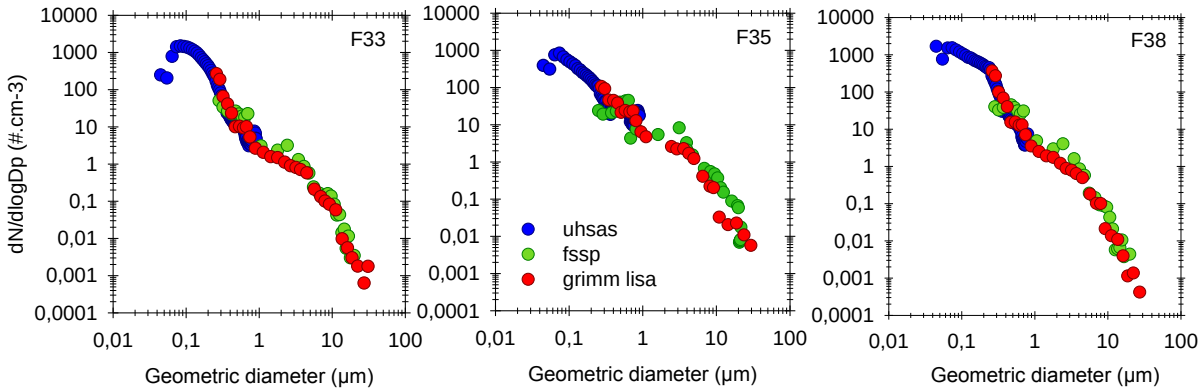

Figure A. Comparison of the number size distributions measured by the UHSAS, FSSP and GRIMM within different dust layers during the campaign.

Additional text P21619 L5: During ADRIMED, systematic differences in the size distributions measured by the FSSP-300 and the GRIMM were observed around 2 µm.

R2.14. The authors may be interested in a method of including error bars in refractive-index corrected particle size based on the scattering-size response, which can be represented by freely available software described in Rosenberg et al. (2012) and also discussed in Ryder et al. (2015) and the associated ACPD discussion. This allows the data in the region omitted in this paper to be included, but with appropriate error bars.

As we mentioned above in R2.13., datapoints in the size range where the light intensity response of the instruments would be unique have been removed for data analysis. As a consequence, errors in size distributions are only due to the accuracy of the stepwise variation of the refractive index in the iterative procedure and the measurement uncertainties.

R2.15. Figure 3 – what do the horizontal error bars for FSSP represent? What are the sizing errors for the other instruments?

Horizontal errors bars display the bin sizing uncertainties of the FSSP. The sizing errors for the other instruments are given in section 2.2.1. They are smaller than the size of the symbols in Figure 3.

Additional text: Horizontal errors bars display the bin sizing uncertainties of the instruments.

R2.16. 21620 L1-2 – why was d_{eff} calculated separately for coarse and fine fractions? It would make sense to provide one value for the entire size distribution, or at least to provide this value in the data analysis as well.

The separation of D_{eff} between the coarse and fine modes allows to discriminate if differences in aerosol size distributions within dust plumes are either due to differences in the size/concentration of pollution particles or to differences in the size of mineral dust.

R2.17. Section 2 – what is the instrumental error on the nephelometer and CAPS instrument?

The uncertainties on the nephelometer and CAPS measurements are added.

Additional text P21616 L26: Uncertainty in σ_{scat} measured with the nephelometer is estimated to be 5% (Muller et al., 2011a).

Additional text P21617 L5: Uncertainty in σ_{ext} measured with the CAPS is estimated to be 3% (Massoli et al., 2010).

R2.18. 21620 L18-21 – what were the errors between calculated & measured scattering and extinction of the final values? How many cases were there?

The errors between calculated and measured σ_{scat} and σ_{ext} were 5% and 3%, respectively. This is already stated in section 2.3.: "The calculated values of σ_{scat}(530 nm) and σ_{ext}(530 nm) were compared to that measured by the nephelometer and the CAPS, and values having the closest agreement within the measurement error bars were chosen as the best estimate.".

R2.19. 21621 L1-3 – what is the reference for these cut-offs? If no previous published work is available on these values, data & evidence should be provided here for them.

Information on the modelling and experimental tests performed to characterize sampling inlets are added in the manuscript.

Additional text: The in-aircraft aerosol instruments sampled through isokinetic and isoaxial aerosol inlets. The nephelometer and GRIMM were set up behind the AVIRAD inlet, while the CAPS, SMPS and SP2 were set up behind the Community Aerosol Inlet (CAI). Particle loss can occur both as a result of the inlet aspiration efficiency and the transport losses in the pipework between the inlet and the instruments. The cut-off diameter, at which the passing efficiency of the inlet equals 50%, was determined by a set of wind-tunnel experiments (unpublished data). The passing efficiency was determined as the ratio of the particle number concentration measured by GRIMM optical counters behind the sampling lines of the AVIRAD and CAI inlets to the particle number concentration measured in the main flow of the wing tunnel where the air speed was 93 m s^{-1} as the cruise speed of the ATR-42. Monodisperse polystyrene latex spheres of 0.6, 1.2, 4.6, 7.9 and 11 µm diameter (Duke Scientifics, Thermo Sci.) and polystyrene divinylbenzene spheres of diameter varying between 1 and 35 µm in diameter (also purchased from Duke Scientifics) were first diluted and then put in a reservoir connected to a peristaltic pump. The pump tubing was connected to a pneumatic spinning disk (SPIDI) in order to spray a large amount of droplets from the solution, some droplets having a particle incorporated. An air mover was mounted beneath the SPIDI and thus the droplets were rapidly evaporated. The particle size-dependent passing efficiency of the AVIRAD and CAI sampling inlets shown in Figure S2 indicates that the cut-off diameter value, expressed as optical equivalent, is 12 µm for the AVIRAD inlet and 5 µm for the CAI.

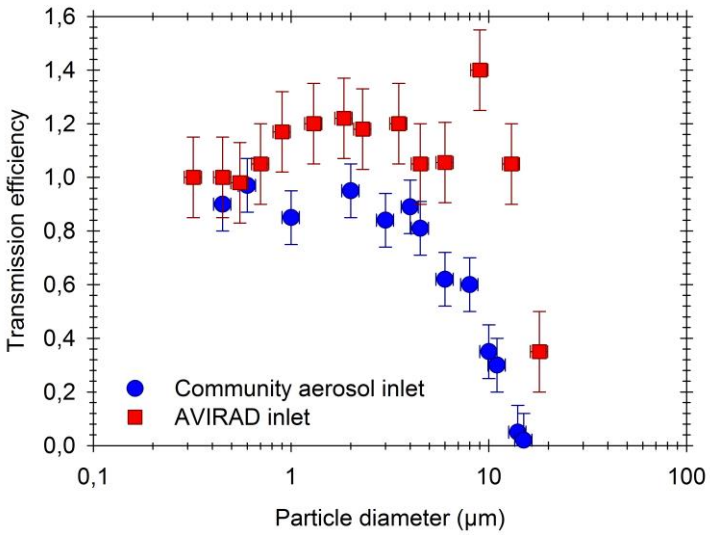

Figure S2. Particle size-dependent passing efficiency of the AVIRAD and CAI sampling inlets.

R2.20. L6-9 – some of these errors, particularly the 0.04 on the single scattering albedo (SSA), are relatively large. The authors say they are within the range covered by the measurement uncertainties, but do not state their values. Therefore the authors should provide values for measurement uncertainty of scattering and extinction, and on SSA as a result.

Measurement uncertainties of scattering and extinction coefficients are added in the text. Please look at our response to comment R2.17 above.

R2.21. Section 2, inlets

More discussion of this point is required. Firstly the GRIMM is measuring a size distribution behind the AVIRAD inlet with a 12 micron cut-off, yet the authors present a size distribution from this inlet up to a nominal size of 32 microns, and what looks like a corrected size of around this value in Fig 3b. If the cut-off value of the inlet is accurate, then the size distribution beyond 12 microns should not be used. Secondly the nephelometer also measures behind the AVIRAD instrument, cutting off at 12 microns, while the CAPS measures extinction behind the community inlet cutting off at 5 microns. This difference should be stated explicitly. How do the authors deal with this discrepancy, e.g. in calculating SSA and in comparing to the mie calculations from the size distributions? A short description of this is provided but it needs more explanation & description of their method.

GRIMM size distributions above the nominal diameter of 12 µm are removed from data analysis to simplify the methodology section.

The fact that the instruments sampled through two different inlets is now clearly stated in the manuscript (please look at R2.19 for further information). We provide additional explanation of the method used to estimate the errors associated with the calculated optical parameters due to the inlets passing efficiencies.

Additional text P21620 L22: To assess the impact of the inlets sampling efficiency on the measured optical properties, Mie scattering calculations were performed to estimate n_r, n_i, ω_0, g and k_{ext} using either the full size distribution or the size distribution measured behind the aircraft inlets. For ω_0, g and k_{ext}, we considered a fixed refractive index of 1.52-0.003i, reflective of the values observed for Saharan dust in source region (Schladitz et al.,

2009; Formenti et al., 2011a; Ryder et al., 2013a). The discrepancies between ω_0, g and k_{ext}, including or not larger particle sizes were used to estimate the errors associated to the inlets sampling efficiency. For n_r and n_i, we estimated the difference between ñ derived from the iterative procedure described above (i.e. Fig. 2) using the full size distribution as input parameter and that obtained from the size distribution measured behind the aircraft inlets. The absolute errors associated with ω_0, g and k_{ext} due to the passing efficiencies of the inlets were in the range covered by the measurements uncertainties of both optical parameters and size distributions, which were estimated to be 0.02, 0.002, 0.04, 0.05 and 0.08, respectively.

R2.22. 21662 L1-12 – could the dust masses also be tracked via the SEVIRI imagery, and were they in agreement with the age and source locations from HYSPLIT?
Dust source regions and transport pathways identified from HYSPLIT were confirmed by SEVIRI observations, as well as by the quantification of Si/Al and Fe/Ca ratios. Information on the method and the uncertainties in identifying dust source regions and age are already given in sections 2.4. and 3.4, respectively.

R2.23. 21622 L19 – 700hPa is more mid-atmosphere than 'upper' atmosphere.
This is corrected.

R2.24. Figure 1 – the squares give the impression that the source regions were very definite and refined. In reality this is probably quite unlikely given the uncertainty in hysplit back trajectories. Please give some measure of spatial uncertainty for each of the sources. Several tools such as ensembles and matrices are now available on HYSPLIT to provide such information easily.
A discussion on the uncertainties of our identification of dust source region is already given in section 3.4.

R2.25. Figure S4 – it is extremely difficult to make out the wind barbs from these plots. Please improve the readability of the figure – I suggest plotting fewer wind barbs.
Figures S4 and S5 have been replotted with fewer wind barbs to improve their readability.

R2.26. 21624 L10 – what method was used to calculate the value of Zb? Was it done by eye? Likewise for Zs. What do you use Zs to infer? Looking at the profiles in Fig S6, it would often appear that Zb should be at a lower altitude on some occasions – e.g. around 300m in F32 rather than 1km. Likewise, the reason for the altitude of the zs line is not clear, for example in F30 and F31 there is little change in wind direction at the line. Please provide information on how Zb and Zs were chosen. This has been done previously in a systematic way, for example, in E.Jung et al., 2013, JGR, oi:10.1002/jgrd.50352, where layers are referred to as 'marine boundary layer,' 'intermediate layer,' and 'Saharan air layer.'
Thank you for this comment. Figures 5 and S6 have been corrected accordingly.
The method used to identify Zb and Zs is provided in P21624 L13: "The top height of the boundary layer was identified as the height at which the temperature profile showed the highest discontinuity and the water vapor mixing ratio decreased the most rapidly. The shear level was determined from the sudden increase in wind speed and change in wind direction. »

R2.27. Fig S6 – both the blue lines appear similar in colour (different shades of dark blue). Please change the colour. Potential temperature axis is not readable due to too many numbers on the x-axis.

The colour code and the scale of the potential temperature axis are changed.

R2.28. 21625 L4 – F31 does not appear to be a single homogeneous layer.

Both total number concentration and Angstrom exponent stayed rather constant with the altitude in F31. There was also no clear evidence from wind speed and direction of the presence of two distinct elevated layers.

R2.29. L10 – McConnell et al. (2008) angstrom values were >0 over the source region (figs 5a and c)

Yes, McConnell angstrom values were >0 but they were also <0.5. They did not reach the value of 0.9 that we obtained during F38.

R2.30. Fig 6 – One would assume that the locations of the profiles in Fig 5 correspond to the stars in fig 1. I.e. expect the F32 profile to be at Minorca. The F38 track is not visible on Fig1. Why then do the end points of the trajectories in Fig 6 not correspond to the profile locations?

The F38 profile was located at Lampedusa (i.e. Table 1) that corresponds well to the localisation of the end point of the trajectory in Figure 6. The colour code of flights tracks in Fig. 1 is modified to make them more visible.

R2.31. Figure 7 – have the categories shown here been created purely based on the altitude of measurement, or do they relate to the placing of lines zb and Zs in Fig 5 in any way?

The classifications were derived from the altitude of measurement. This is already written in the caption of the figure: "Size distributions are classified as a function of the altitude of the layer: elevated dust layer above 3 km a.s.l. (red), intermediate dust layer between 1.5–3 km a.s.l. (blue) and the boundary layer below 1 km (green)."

R2.32. 21627 L4 – 'indiscriminate of'?

Thank you, this is corrected.

R2.33. L4-6 – it is surprising that the intermediate dust shows a greater coarse mode than the elevated dust – based on Fig 5 it seems that there were more coarse particles in the elevated layer. It would be useful to show Fig 7 a and b normalized by total number and volume respectively, so that the relative differences in size distribution can be seen. Then fig 7c could be shown as a separate figure, enlarged for clarity – it is quite difficult to see some of the detail and different lines here.

It can be seen in Figure 9 that the differences in the coarse mode between the two elevated dust layers stayed within the measurement error bars, so the variation is most likely not significant. The relative differences in size distributions are already discussed in section 4.1. and can be seen from the vertical variation of D_{eff} shown in Figure 9.

R2.34. L22 – what do you mean by 'good'?

This is clarified in the text.

Additional text: The spread of volume size distributions obtained during ADRIMED overlaps with those measured during other airborne campaigns close to dust source regions (AMMA, FENNEC and SAMUM-1) in the coarse mode size range (Figure 7c).

R2.35. L23 – Please clarify what is meant by Deff,c here – is this deff of particles d>1 micron, or deff of mode 4 in table 3?

The definition of $D_{eff,c}$ is now reminded in this section.

Updated text: "Effective diameters of the coarse mode $D_{eff,c}$ (i.e. estimated in the size 1-32 µm as defined in eq. 7) ranged from 3.8 to 14.2 µm during ADRIMED"

R2.36. L27 – 'uncounted' – do you mean, 'fewer particles larger than 10 um were counted'?

Yes, thank you.

R2.37. Figure 8 – presumably one SLR equates to one data point. How do you deal with data from the vertical profiles? Are they averaged over an altitude range depending on the vertical structure? What do the error bars represent?

The altitude used to plot the data points is already given in the caption: "The altitude indicated for vertical profiles refers to the middle of the layer".

A description of the error bars has been added in the caption.

Additional text: Horizontal error bars display the uncertainties of the parameters. Vertical error bars indicate the altitude range used to calculate each data point.

R2.38. Figure 8 – adding in horizontal lines at 1.5 and 3km to represent and differentiate the different dust altitude categories shown in Fig 7 would be useful. It would also be useful to add in some measure of size as an extra plot – e.g. ratio of Ncoarse to Nfine, or deff coarse/deff fine.

Horizontal lines are added in Figure 8 to differentiate the elevated and intermediate dust layers. We have the impression, however, that representing the vertical distribution of either N_c/N_f or $D_{eff,c}/d_{eff,f}$ would not help to improve our understanding of the evolution of dust size distribution since we would not be able to discriminate if variations are due to differences in the size/concentration of pollution particles or to differences in the size /concentration of mineral dust.

R2.39. 21629 L9 – 'these layers' – do you mean the higher altitude layers?

Yes, this is clarified.

Updated text: As ñ was found to be constant with the altitude (i.e. Figure 8a-b), these variations in g and k_{ext} were probably due to the variability in particles size distributions, which is consistent with the larger fraction of fine particles found in the higher altitude dust layers.

R2.40. L1-14 – the variation of optical properties with height is worthy of a bit more discussion. It appears that nr and ni are independent of altitude, there is some evidence for a decrease in SSA beneath 3km, and beneath 3km g decreases while kext increases. The latter (g and kext) are consistent with an increase in the proportion of accumulation mode particles relative to the coarse particles – which is why it would be useful to add a size metric to this figure.

Even if the vertical variability of the optical parameters were most likely related to differences in dust size distributions, we do not believe that this result deserves further discussion. Differences in g, k_{ext} and $D_{eff,c}$ between the intermediate and elevated dust

layers were low and statistically not significant regarding corresponding error bars. Therefore we would prefer not expend this discussion in the paper.
The discussion on the vertical variation of optical parameters mentioned by Reviewer #2 is already provided in the paper.: "Only slightly low values of g (from ~ 0.7 to ~ 0.8) and k_{ext} (from ~ 0.3 to ~ 0.7 m g) were observed for some dust layers below 3 km a.s.l. As ñ was found to be constant with the altitude (i.e. Fig. 8a and b), these variations in g and k_{ext} were probably due to the variability in particles size distributions, which is consistent with the larger fraction of fine particles found in these dust layers (i.e. Fig. 7a)."
Moreover, the vertical distribution of the size distribution can already be seen in Figures 7 and 9.

R2.41. 21630 L2-5 – There is not strong evidence here that the transport conditions affect the optical properties of the dust layer – in fact based on Fig 8 and the discussion in the preceding paragraphs of the paper, I would argue the opposite. The results presented here would suggest that transport altitude/air mass encounters affects the resulting vertical structure, but I would be doubtful if more than that can be claimed. Additionally, nothing is known about the dust size distribution or optical properties at uplift, which may have been different in each case.
Our conclusions on dust optical properties referred to observations conducted from remote-sensing techniques and presented below in the paragraph. To avoid any confusion, the end of the paragraph is modified to better support the conclusions drawn from our observations.
Updated text: Overall, these contrasting results highlight the major role of the transport conditions (height, air mass encountered) of the dust plumes in governing the mixing processes of mineral dust with other aerosol species.

R2.42. 21630 L17- do you mean 'upper 3km'? If not please define what sort of size you mean when referring to 'pollution particles.' Again, it may be helpful to the reader here to include some measure of number concentration in the figure (e.g. ratio of N coarse/Nfine, or sub-divide the fine mode into ratio of number concentrations).
No, "lower 3 km" is right. It can be seen in the higher proportion of fine mode particles in the lower 3 km altitude. Please look at our responses of R2.16 and R2.33 concerning $D_{eff,c}/D_{eff,f}$.

R2.43. L25-26 – 'Deff,c of the dust plume did not show any systematic dependence on altitude' – on the contrary there does seem to be a small shift to smaller values of deff above 3km. What are the mean & standard deviation values of deff in these 2 altitude ranges, and can you provide evidence that there is no systematic change?
Please look at our response to R2.41.

R2.44. Figure 10 – please include deff for the coarse mode in this figure or supply 2 plots to include it. Due to the limited settling velocity of fine mode particles, deff,f would not be expected to change much on the timescales shown, whereas deff,coarse might be expected to change significantly.
The time evolution of $D_{eff,c}$ is presented in Figure 11 to investigate the effect of sedimentation processes on the proportion of large particles in dust size distributions. The aim of Figure 10 is to explore the role of the transport time of the dust plumes on their mixing rate with pollution particles. Despite the export of pollution particles within dust

layers up to 3 km altitude, $D_{eff,c}$ did not vary substantially with altitude (Figure 9b) due to the external mixing of mineral dust with pollution. So we do not believe that it would be relevant to show the time evolution of $D_{eff,c}$ for the intermediate and elevated dust layers in this section.

R2.45. 21632 L26 – a value of 0.64 for k_{ext} seems at the high end compared to values shown in Fig 8e. How do the authors reconcile the choice of this value? What are the uncertainties on the SSA values calculated from the chemical composition?

The k_{ext} value of 0.64 recommended by OPAC is indeed among the highest values obtained during ADRIMED. Dust absorption depends on the dust mineralogical composition and hence can vary with dust source region. The OPAC parametrization consists of a heterogeneous mixture of quartz and clay minerals originating from different sources. As a result the default OPAC's type mineral dust could slightly differ from dust sampled during ADRIMED and this could result in some differences in k_{ext} values of dust at emission. Without proper measurements of dust properties at uplift, we can only speculate on that issue and we decided to assume an average k_{ext} value of dust at emission as provided in OPAC dataset. It is also worth noting that this average value remain within the range of values retrieved during ADRIMED.

To estimate the uncertainties on the SSA calculated from the chemical composition would require to know the uncertainties on k_{ext}. As mentioned above, without measurements of dust plume at uplift, we decided to use an average k_{ext} value from OPAC. Unfortunately the uncertainty of this parameter is not provided. However SSA obtained from chemical composition ranged from 0.93-0-97 which falls within the range of values obtained from optical measurements (0.92–0.99 ± 0.04). Our calculation is thus conclusive without knowing SSA uncertainties.

R2.46. Can the chemical data provide any information on composition as a function of size? For example, generally the authors assume that dust is present at all particle sizes and subsequent conclusions (e.g. Fig 10 is discussed as dust, albeit being fine mode). What evidence is there that dust is present in all size ranges? Likewise, can the chemical data be used to support the conclusion that more pollution was present in intermediate compared to elevated dust layers?

Analysis of size segregated sampling by electron microscopy is planned to address more specifically this point, whereas the chemical analysis available at this stage are size-integrative. However, there is clear evidence from the aerosol size distribution (i.e. Figure 7) of the presence of fine dust particles within the dust layers (section 3.3) in agreement with earlier work in proximity of source regions (Chou et al., 2008: McConnell et al., 2008; Kandler et al., 2009). Indeed a peak in the accumulation mode similar as that observed in dust source region and not present in the MBL (Figure 7) suggests the presence of dust particles in the fine mode.

R2.47. Figure 11 – Please clarify how effective diameter is provided for each dataset in the figure. For example, the Fennec data represent effective diameter for the full size distribution. It is likely the case for the other campaigns. Therefore it would be better to show the ADRIMED data as deff for the full size distribution in order to compare like with like. Additionally it should be noted that the other campaign data points are averages of many individual cases, while the ADRIMED data points each represent 1 SLR (?) (or profile?). This is appropriate due to the

focus of this paper on the ADRIMED measurements, but the authors should also provide one mean data point for the campaign with error bars so that it can be easily represented in future studies/publications. This is useful and important data and it should be provided in a way that allows it to be taken forward easily.

Since the aim of Figure 11 is to investigate the evolution of large dust particles with time, we would prefer to present D_{eff} for the coarse mode only. D_{eff} for the coarse mode has been calculated from the number size distribution and using equation (7) for ADRIMED, AMMA, SAMUM 1,2 and PRIDE datapoints. For Fennec, we mistakenly used D_{eff} provided in Figure 11 of Ryder et al. (2013) that referred actually to the full size distribution. Figure 11 is now corrected accordingly. Moreover, a mean data point for the ADRIMED campaign is added in the figure.

R2.48. 21634 L10-14 – can the authors speculate on whether this is greater than expected up/downdraft values over the Atlantic, and whether this might also help explain (or not) why Fig 11 intriguingly suggests that larger particles are transported over the Mediterranean more effectively than over the Atlantic?

To the best of our knowledge, no study to date has explored possible differences in the thermal turbulence within layers circulating over the Atlantic and the Mediterranean basin. This research topic should clearly be investigated in the future to better understand the differences in the sedimentation of large Saharan dust particles during these two main transport pathways and to improve the representativeness of the temporal evolution of dust size distribution in models.

Final comments:

R2.49. What were the AODs of the sampled cases? What were the AODs in the polluted regions out of dust plumes? (I.e. how strong were levels of background pollution?) Since the pollution appears to have negligible effect on the dust properties, it would be useful to know whether this is because pollution levels were low in general in the area/time period, or conversely if loadings of pollution were moderate-high, and still not impacting the dust layer properties. I see this is discussed briefly in the conclusion but it would merit a mention in the results section as well.

A short paragraph on the representativeness of our results including AOD values is added in the text.

Additional text P21632 L7: The ADRIMED field campaign was characterized by moderate aerosol optical depth (AOD) with averaged values ranging between 0.1 – 0.6 at 440 nm as observed by AERONET/PHOTONS sun-photometers (see Figure 19 of Mallet et al., 2015). Outside of dust events, the AOD displayed values from 0.1 to 0.2 (440 nm), while it reached values up to 0.8 under dusty conditions. Although higher AOD values have already been observed in the Mediterranean region during intense pollution or biomass burning events (Pace et al., 2005; Alados-Arbodelas et al., 2011), values obtained during ADRIMED are typical of those observed in summertime (Nabat et al., 2015). This observation is also supported by the mass concentration of the main anthropogenic compounds that reached typical values for the region, as discussed previously. Our result on the moderate absorption properties of the dust plumes is thus likely relevant to dust events in the western Mediterranean in the absence of intense pollution or biomass burning emissions and can be used for constraining modeling studies and satellite retrievals that make assumption on dust optical properties.

References:

Alados-Arboledas, L., Müller, D., Guerroro-Rascado, J. L., Navas-Guzman, D. Pérez-Ramirez, D., and Olmo, F. J. : Optical and microphysical properties of fresh biomass burning aerosol retrieved by Raman lidar, and star-and sun-photometry, Geophys. Res. Lett., 38, L01807, doi:10.1029/2010GL45999.

Baumgardner, D., Dye, J. E., Gandrud, B. W., and Knollenberg, R. G.: Interpretation of measurements made by forward scattering probe (FSSP-300) during the airborne arctic stratospheric expedition, J. Geophys. Res.-Atmos., 97, 8035-8046, 1992.

Chou, C., Formenti, P., Maille, M., Ausset, P., Helas, G., Harrison, M., and Osborne, S.: Size distribution, shape, and composition of mineral dust aerosols collected during the African Monsoon Multidisciplinary Analysis Special Observation Period 0: Dust and Biomass-Burning Experiment field campaign in Niger, January 2006, J. Geophys. Res.-Atmos., 113, D00C10, 10.1029/2008JD009897, 2008.

Formenti, P., Rajot, J. L., Desboeufs, K., Saïd, F., Grand, N., Chevaillier, S., and Schmechtig, C.: Airborne observations of mineral dust over western Africa in the summer Monsoon season: spatial and vertical variability of physico-chemical and optical properties, Atmos. Chem. Phys., 11, 6387-6410, 10.5194/acp-11-6387-2011, 2011a.

Kandler, K., SchÜTz, L., Deutscher, C., Ebert, M., Hofmann, H., JÄCkel, S., Jaenicke, R., Knippertz, P., Lieke, K., Massling, A., Petzold, A., Schladitz, A., Weinzierl, B., Wiedensohler, A., Zorn, S., and Weinbruch, S.: Size distribution, mass concentration, chemical and mineralogical composition and derived optical parameters of the boundary layer aerosol at Tinfou, Morocco, during SAMUM 2006, Tellus B, 61, 32-50, 10.1111/j.1600-0889.2008.00385.x, 2009.

Mallet, M., Dulac, F., Formenti, P., Nabat, P., Sciare, J., Roberts, G., Pelon, J., Ancellet, G., Tanré, D., Parol, F., di Sarra, A., Alados, L., Arndt, J., Auriol, F., Blarel, L., Bourrianne, T., Brogniez, G., Chazette, P., Chevaillier, S., Claeys, M., D'Anna, B., Denjean, C., Derimian, Y., Desboeufs, K., Di Iorio, T., Doussin, J. F., Durand, P., Féron, A., Freney, E., Gaimoz, C., Goloub, P., Gómez-Amo, J. L., Granados-Muñoz, M. J., Grand, N., Hamonou, E., Jankowiak, I., Jeannot, M., Léon, J. F., Maillé, M., Mailler, S., Meloni, D., Menut, L., Momboisse, G., Nicolas, J., Podvin, J., Pont, V., Rea, G., Renard, J. B., Roblou, L., Schepanski, K., Schwarzenboeck, A., Sellegri, K., Sicard, M., Solmon, F., Somot, S., Torres, B., Totems, J., Triquet, S., Verdier, N., Verwaerde, C., Wenger, J., and Zapf, P.: Overview of the Chemistry-Aerosol Mediterranean Experiment/Aerosol Direct Radiative Forcing on the Mediterranean Climate (ChArMEx/ADRIMED) summer 2013 campaign, Atmos. Chem. Phys. Discuss., 15, 19615-19727, 10.5194/acpd-15-19615-2015, 2015.

Muller, T., Laborde, M., Kassell, G., and Wiedensohler, A.: Design and performance of a three-wavelength LED-based total scatter and backscatter integrating nephelometer, Atmos. Meas. Tech., 4., 1291-1303, doi:10.5194/amt-4-1291-2011, 2011a.

Massoli, P., Kebabian, P. L., Onasch, T. B., Hills, F. B., and Freedman, A., Aerosol light extinction measurements by Cavity Attenuated Phase Shift (CAPS) Spectroscopy: Laboratory validation and field deployment of a compact aerosol particle extinction monitor, Aerosol Sci. Tech., 44:6, 428-435, DOI:10.1080/02786821003716599, 2010.

Nabat, P., Solmon, F., Mallet, M., Michou, M., Sevault, F. Driouech, F., Meloni, D., di Sarra, A., Di Biagio, C., Formenti, P., Sicard, M., Léon, J.-F., and Bouin, M. -N.: Dust aerosol radiative effects during summer 2012 simulated with a coupled regional aerosol-

atmosphere-ocean model over the Mediterranean, Atmos. Chem. Phys., 15, 3303-3326, doi:10.5194/acp-15-3303-2015, 2015.

Pace, G., Meloni, D., and di Sarra, A.: Forest fire aerosol over the Mediterranean basin during summer 2003, J. Geophys. Res., 110, D21202, doi:10.1029/2005JD005986, 2005.

Ryder, C. L., Highwood, E. J., Lai, T. M., Sodemann, H., and Marsham, J. H.: Impact of atmospheric transport on the evolution of microphysical and optical properties of Saharan dust, Geophys. Res. Lett., 40, 2433-2438, 10.1002/grl.50482, 2013a.

Schladitz, A., Muller, T., Kaaden, N., Massling, A., Kandler, K., Ebert, M., Weinbruch, S., Deutscher, C., and Wiedensohler, A.: In situ measurements of optical properties at Tinfou (Morocco) during the Saharan Mineral Dust Experiment SAMUM 2006, Tellus B, 61, 64-78, 10.1111/j.1600-0889.2008.00397.x, 2009.